

Measurement of Apparent Diffusion Coefficient (ADC) Values of Ependymoma and Medulloblastoma Tumors: a Patient-based Study

Taheri H.¹, Tavakoli M. B.^{2*}

ABSTRACT

Background: Some brain tumors such as ependymoma and Medulloblastoma have similar MR images which may result to undifferentiated them from each other.

Objective: This study aimed to compare the apparent diffusion coefficient (ADC) of two different cerebellar pediatric tumors, including ependymoma and medulloblastoma which have shown similar clinical images in conventional magnetic resonance imaging (MRI) methods.

Material and Methods: In this analytical study, thirty six pediatric patients who were suspected to have the mentioned tumors according to their CT image findings were included in this study. The patients were subjected to conventional MRI protocols followed by diffusion weighted imaging (DWI) and ADC values of the tumors were calculated automatically using MRI scanner software.

Results: The mean (\pm SD) ADC value for ependymoma ($1.2 \pm 0.06 \times 10^{-3}$ mm²/s) was significantly higher than medulloblastoma ($0.87 \pm 0.02 \times 10^{-3}$ mm²/s) ($p = 0.041$). Moreover, the maximum ADC value of ependymoma was considerably different in comparison with medulloblastoma (1.4×10^{-3} mm²/s and 0.96×10^{-3} mm²/s, respectively; $p = 0.035$). Furthermore, the minimum ADC value of ependymoma was higher compared to medulloblastoma (1.0×10^{-3} mm²/s and 0.61×10^{-3} mm²/s, respectively), but there was not significant ($p = 0.067$).

Conclusion: Evaluation of ADC values for ependymoma and medulloblastoma is a reliable method to differentiate these two malignancies. This is due to different ADC values reflected during the evaluation.

Citation: Taheri H, Tavakoli MB. Measurement of Apparent Diffusion Coefficient (ADC) Values of Ependymoma and Medulloblastoma Tumors: a Patient-based Study. *J Biomed Phys Eng*. 2021;11(1):39-46. doi: 10.31661/jbpe.v0i0.889.

Keywords

ADC; DWI; Magnetic Resonance Imaging; Pediatric Tumors; Medulloblastoma; Ependymoma

Introduction

For malignancies and lesions conventional magnetic resonance imaging techniques such as axial contrast enhancement T₁ weighted (T₁W), axial T₂ weighted (T₂W), and also axial fluid attenuated inversion recovery (FLAIR) are considered as the most common diagnostic choices, whereas a number of studies have been shown that diffusion weighted imaging (DWI) has opened new horizons on the differentiation of some brain tumors and provided additional information about microscopic motion of the water proton depending on the thermal energy of tissues [1-7]. According to many studies, tumors and lesions

¹MSc, Department of Medical Physics, School of Medicine, Isfahan University of Medical Sciences, Isfahan, Iran
²PhD, Department of Medical Physics, School of Medicine, Isfahan University of Medical Sciences, Isfahan, Iran

*Corresponding author:
M. B. Tavakoli
Department of Medical Physics, School of Medicine, Isfahan University of Medical Sciences, Isfahan, Iran
E-mail: mbtavakoli@mui.ac.ir

Received: 12 January 2018
Accepted: 14 March 2018

may have different apparent diffusion coefficient (ADC) maps, as a result of variations in the amount of water diffusivity, and using DWI can be a good choice to differentiate similar lesions from each other [8-11]. Several studies have demonstrated that the differentiation between some pediatric brain tumors such as ependymoma and medulloblastoma may be difficult with the stated conventional protocols in clinical situation [12, 13]. This study aimed to compare the ADC values of two different pediatric cerebellar tumors, namely ependymoma and medulloblastoma with the hypothesis that their ADC values may allow differentiation of the mentioned tumors on the diffusion weighted MR images.

Material and Methods

A. Patient Selection

The analytical study was performed in the medical physics department of Isfahan University of Medical Sciences, Isfahan, Iran from 2011 to 2017. It is included 36 patients (21 males and 15 females) who referred from the Sayed Al Shohada hospital cancer center (Isfahan, Iran) to a medical image center. All of them (age range 4 to 9 years old) were suspected to have ependymoma and medulloblastoma according to their CT image findings.

B. MR Imaging

The MRI studies were performed using a 1.5 Tesla Philips MRI scanner with protocols, including non-contrast T_1W images in axial and sagittal planes (TR/TE: 4400/110 ms, NEX = 1, 220 mm field of view (FOV), 5 mm slice thickness, 1 mm interslice gap), post contrast axial, coronal and sagittal T_1W images (TR/TE: 4400/110 ms, NEX = 1, 220 mm FOV, 5 mm slice thickness, 1 mm interslice gap), and also axial and sagittal T_2W images (TR/TE: 4400/110 ms, NEX = 1, 220 mm FOV, 5 mm slice thickness, 1 mm interslice gap).

The DWI sequences were done according to Figure 1. As illustrated in Figure 1, two strong diffusion-sensitizing gradients (DG's) were exerted on both sides of the 180° -pulse. The DG pair did not affect the phase of the stationary spins since phase accumulation by the first gradient lobe was followed by the second one, as a reverse. However, diffusing spins were moved into different locations existed between the first and second lobes resulting in falling out of phase and losing signal. Instantly, an image acquisition module was played out following the second DG. This is typically an echo-planar sequence that generates multiple gradient echoes by rapidly oscillating phase and frequency gradients. In order to decrease the chemical shift artifacts, all commercial

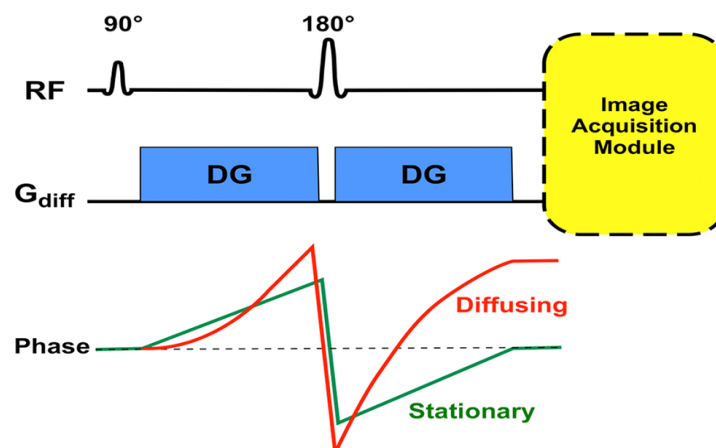


Figure 1: Diagram of diffusion weighted magnetic resonance (MR) imaging diffusion weighted image (DWI).

DWI sequences utilized suppression of some sorts of fat in the image. This can be a chemically-selective fat saturation pulse or a nonselective “STIR-like” inverting pulse applied immediately before the 90°-pulse. Alternatively, as another phenomenon, water protons were solely excited by a selectively tuned 90°-pulse. To suppress eddy currents and reduce spatial distortion, a second 180°-refocusing pulse was made just before beginning of the image acquisition module [14-16]. The used DWI was included a multi-section single shot spin echo EPI sequence (TR/TE: 4400/110 ms, NEX =1) with diffusion sensitivities of b values = 1000 s/mm². The diffusion gradients were applied sequentially in X, Y and Z directions. The slice thickness and inter-slice gap were 5 mm and 1 mm, respectively. The FOV was chosen 240 mm and the matrix size was 256× 256 for all images. The total acquisition time for each patient was 80 s.

The enhancing solid portion of stated lesions was identified on post-contrast T₁W images and the matching ADC maps for each patient. Regions of interest (ROIs) were drawn in the ADC maps and the ADC values were calculated automatically by a MRI scanner software (were expressed in 10⁻³ mm²/s) according to the following equation [14-16]:

$$S / S_0 = e^{-bD}$$

Where, S is the diffusion-weighted signal, S₀ is the signal intensity without the diffusion weighting, b is the diffusion sensitivity (b-value), and D is the diffusion coefficient (ADC value).

C. Statistical analysis

Mean values and standard deviations of the ADC values for ependymoma and medulloblastoma were calculated and statistical significance of the differences between them was evaluated. A computer software (SPSS version 16.0, Chicago, IL, USA) was used for statistical analysis. Data were analyzed using Wilcoxon test (Nonparametric version of paired samples T- test). All hypotheses were tested

using a criterion level of P = 0.05.

Results

Figures 2 and 3 illustrate the post contrast enhanced T₁W, and T₂W images of the ependymoma and medulloblastoma. Figure 4 shows the ADC maps of the stated malignancies. Table 1 indicates the measured ADC values of different patients included in the study. Table 2 shows the maximum, mean and minimum ADC values of ependymoma and medulloblastoma. Figure 5 gives a comparison between the ADC ranges of tumors studied.

According to Table 2, the mean (± SD) ADC value for ependymoma was 1.2± 0.06 ×10⁻³ mm²/s. The maximum and minimum ADC values of ependymoma were 1.4 ×10⁻³ mm²/s and 1.0 ×10⁻³ mm²/s, respectively (Table 2 and Figure 5).

Whereas the mean (± SD) ADC value was 0.87 ± 0.02 ×10⁻³ mm²/s (Table 2) for the medulloblastoma. It was found that the maximum and minimum ADC values of medulloblastoma were 0.96×10⁻³ mm²/s and 0.61×10⁻³ mm²/s, respectively (Table 2 and Figure 5).

Discussion

Diffusion weighted imaging (DWI) is widely used to investigate cerebral lesions such as infarction, abscess, multiple sclerosis (MS) and also differentiate similar tumors and malignancies from each other [12, 17, 18]. Furthermore, it is a suitable protocol which can illustrate high quality images from tumors without using image contrast enhancement materials which are commonly used in conventional protocols such as T₁W and T₂W images. Therefore, the study was performed to measure the ADC values of two different pediatric tumors, including ependymoma and medulloblastoma illustrating similar clinical images in conventional techniques and also differentiating them from each other may be difficult in clinical situation.

Table 2 and Figure 5 gives the comparison of ADC values among the stated tumors. Our

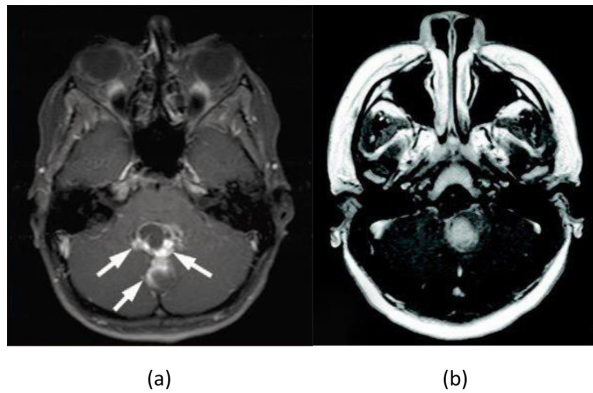


Figure 2: The post contrast enhanced T_1W images of ependymoma (a) and medulloblastoma (b).

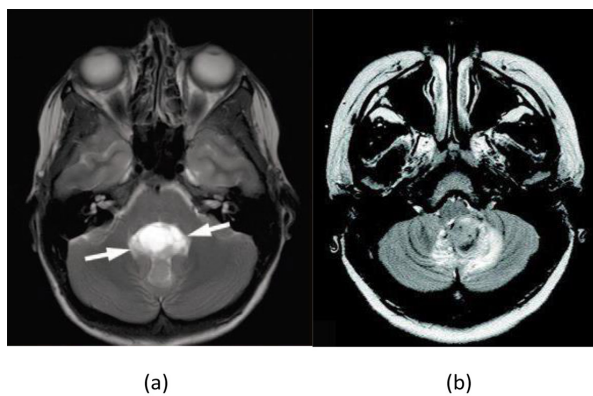


Figure 3: The axial T_2W images of ependymoma (a) and medulloblastoma (b).

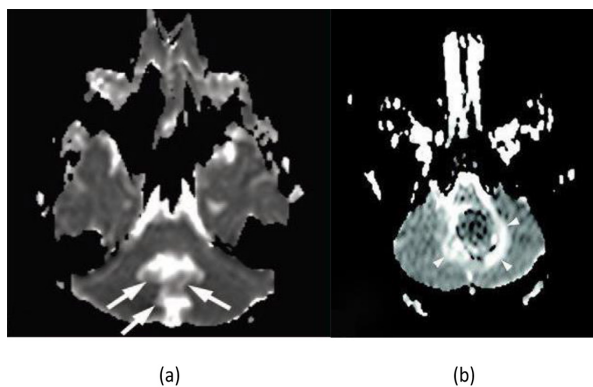


Figure 4: The apparent diffusion coefficient (ADC) maps for ependymoma (a) and medulloblastoma (b).

Table 1: Measured apparent diffusion coefficient (ADC) values for ependymoma and medulloblastoma in different patients who included in the study. The values are expressed in $10^{-3} \text{ mm}^2/\text{s}$.

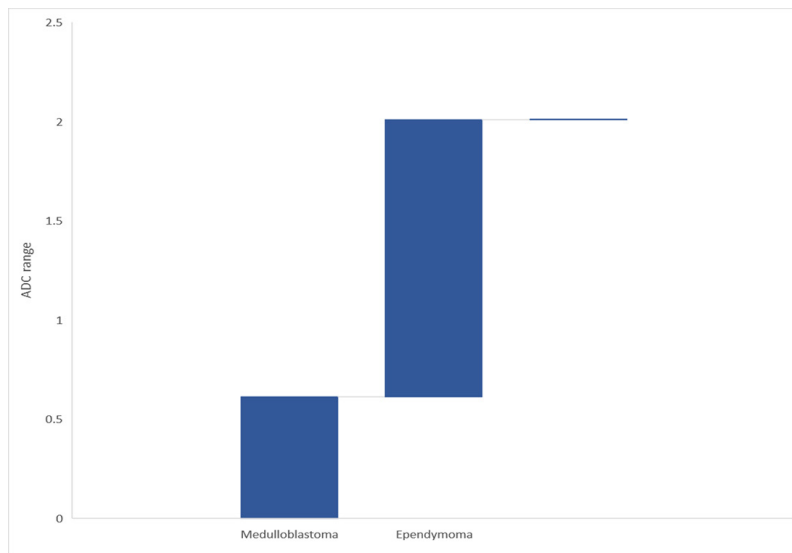
Patient number	Ependymoma (ADC value)	Medulloblastoma (ADC value)
1	1.0	---
2	1.3	---
3	1.2	---
4	1.0	---
5	1.0	---
6	1.1	---
7	1.4	---
8	1.1	---
9	1.0	---
10	1.3	---
11	1.2	---
12	1.1	---
13	1.3	---
14	1.0	---
15	1.3	---
16	1.4	---
17	1.1	---
18	1.0	---
19	1.2	---
20	1.1	---
21	1.2	---
22	1.4	---
23	---	0.75
24	---	0.61
25	---	0.88
26	---	0.64
27	---	0.67
28	---	0.83
29	---	0.74
30	---	0.90
31	---	0.72
32	---	0.64
33	---	0.71
34	---	0.89
35	---	0.96
36	---	0.82

ADC: Apparent diffusion coefficient

Table 2: Multiple comparisons among the apparent diffusion coefficient (ADC) values of ependymoma and medulloblastoma.

	Ependymoma	Medulloblastoma	Adjusted p value
Maximum ADC value ($\times 10^{-3}$ mm²/s)	1.4	0.61	0.035
Mean ADC value ($\times 10^{-3}$ mm²/s)	1.2 \pm 0.06	0.87 \pm 0.02	0.041
Minimum ADC value ($\times 10^{-3}$ mm²/s)	1.0	0.96	0.067

ADC: Apparent diffusion coefficient

**Figure 5:** The apparent diffusion coefficient (ADC) ranges (in 10^{-3} mm²/s) among the studied tumors.

data showed that ADC values were different between the studied malignancies. According to the results, it was found that ADC values also clearly distinguished medulloblastoma from ependymoma in all patients without having any overlap.

Based on the results, the maximum and mean ADC values of ependymoma were significantly different compared to medulloblastoma ($p = 0.035$ and $p = 0.041$, respectively). In addition, the minimum ADC value for ependymoma was higher than medulloblastoma while it was not significant ($p = 0.067$). This was seen due to higher water diffusivity of ependymoma in comparison with medulloblastoma that may lead to higher ADC values for ependymoma in comparison with medulloblastoma [14-16, 19]. Moreover, it is known that thermal en-

ergy can significantly affect the water movement [7, 9-11]. Therefore, it is considered that thermal energy of ependymoma may be higher than medulloblastoma which can make higher motion of the water proton in ependymoma in comparison with medulloblastoma.

Similar results have been reported in other studies. Mohamed et al., compared the ADC values for ependymoma, medulloblastoma and juvenile pilocytic astrocytoma (JPA) using a 1.5 Tesla MRI scanner. In this study, they found that ependymoma and medulloblastoma have clearly different ADC values and distinguished from each other in all patients without any overlap [20]. Our findings are in an agreement with Rumboldt et al., who stated that ependymomas showed significantly higher ADC values compared to medulloblastomas

($p = 0.0005$) [21]. Fatma et al., reported that evaluation of ADC values for enhancing solid tumors is a simple and reliable method for preoperative differentiation of cerebellar tumors such as ependymoma and medulloblastoma in pediatric patients [22] which is in line with our finding. Recently Zitouni et al., have compared the ADC values of three different pediatric posterior fossa tumors, including JPA, ependymoma and medulloblastoma. In this study, they found ependymoma was differentiated from medulloblastoma with 100% of sensitivity and 88.89% of specificity using an ADC ratio ≤ 1.18 [23]. In the other study, Theodore et al., concluded that the addition of ADC values to standard film interpretation may improve the distinguish rate for the mentioned pediatric tumors [24]. Gauvain et al., reported that using ADC ratio (Tumor ADC: Normal brain ADC) could be a good choice to determine tumor classification [9]. As opposed to these results, Kotsenas et al., concluded that medulloblastoma showed a very hyperintense image on DWI and theorized that the attenuated cellularity of the malignancy may lead to the increased signal intensity. Moreover, it is mostly depended on relatively restricted diffusion [25]. In other study, Jaremko et al., founded that there were three overlap tumors, including a desmoplastic medulloblastoma, an anaplastic ependymoma and a JPA with restricted diffusion in its nodule [26]. Several studies have reported that increasing cellularity may cause signal intensity on DWI, and also hypo intensity on ADC maps of different malignancies to increase [6-9, 27, 28].

According to findings of our study, ependymoma has significantly higher ADC values compared to medulloblastoma due to higher water proton movement and consequently higher water diffusivity.

Conclusion

In this study, the ADC values of two different pediatric malignancies, including ependymoma and medulloblastoma were measured.

Measurement of ADC values for studied tumors could be a suitable alternative to differentiate them from each other due to higher ADC value of ependymoma compared to medulloblastoma.

Acknowledgment

The authors thank Mr. Ehsan Mostajeran for his help in the completion of the article.

Conflict of Interest

None

References

1. Arle JE, Morriss C, Wang ZJ, Zimmerman RA, Phillips PG, Sutton LN. Prediction of posterior fossa tumor type in children by means of magnetic resonance image properties, spectroscopy, and neural networks. *J Neurosurg.* 1997;**86**:755-61. doi: 10.3171/jns.1997.86.5.0755. PubMed PMID: 9126888.
2. Gupta R, Husain N, Kathuria M, Datta S, Rathore R, Husain M, editors. Magnetization transfer MR imaging is more close to histopathology than conventional MR imaging in intracranial tuberculomas. Proceedings of the Eighth Meeting of the International Society for Magnetic Resonance in Medicine Berkeley, Calif: International Society for Magnetic Resonance in Medicine; 2000.
3. Poretti A, Meoded A, Huisman TA. Neuroimaging of pediatric posterior fossa tumors including review of the literature. *J Magn Reson Imaging.* 2012;**35**:32-47. doi: 10.1002/jmri.22722. PubMed PMID: 21989968.
4. Provenzale JM, Mukundan S, Barboriak DP. Diffusion-weighted and perfusion MR imaging for brain tumor characterization and assessment of treatment response. *Radiology.* 2006;**239**:632-49. doi: 10.1148/radiol.2393042031. PubMed PMID: 16714455.
5. Stadnik TW, Chaskis C, Michotte A, Shabana WM, Van Rompaey K, Luypaert R, et al. Diffusion-weighted MR imaging of intracerebral masses: comparison with conventional MR imaging and histologic findings. *AJNR Am J Neuroradiol.* 2001;**22**:969-76. PubMed PMID: 11337344.
6. Sugahara T, Korogi Y, Kochi M, Ikushima I, Shigematu Y, Hirai T, et al. Usefulness of diffusion-weighted MRI with echo-planar technique in

- the evaluation of cellularity in gliomas. *J Magn Reson Imaging*. 1999;**9**:53-60. PubMed PMID: 10030650.
7. Gupta RK, Cloughesy TF, Sinha U, Garakian J, Lazareff J, Rubino G, et al. Relationships between choline magnetic resonance spectroscopy, apparent diffusion coefficient and quantitative histopathology in human glioma. *J Neurooncol*. 2000;**50**:215-26. PubMed PMID: 11263501.
 8. Guo AC, Cummings TJ, Dash RC, Provenzale JM. Lymphomas and high-grade astrocytomas: comparison of water diffusibility and histologic characteristics. *Radiology*. 2002;**224**:177-83. doi: 10.1148/radiol.2241010637.
 9. Gauvain KM, McKinstry RC, Mukherjee P, Perry A, Neil JJ, Kaufman BA, et al. Evaluating pediatric brain tumor cellularity with diffusion-tensor imaging. *AJR Am J Roentgenol*. 2001;**177**:449-54. doi: 10.2214/ajr.177.2.1770449. PubMed PMID: 11461881.
 10. Tien RD, Felsberg GJ, Friedman H, Brown M, MacFall J. MR imaging of high-grade cerebral gliomas: value of diffusion-weighted echoplanar pulse sequences. *AJR Am J Roentgenol*. 1994;**162**:671-7. doi: 10.2214/ajr.162.3.8109520. PubMed PMID: 8109520.
 11. Kono K, Inoue Y, Nakayama K, Shakudo M, Morino M, Ohata K, et al. The role of diffusion-weighted imaging in patients with brain tumors. *AJNR Am J Neuroradiol*. 2001;**22**:1081-8. PubMed PMID: 11415902.
 12. Morriss MC, Zimmerman RA, Bilaniuk LT, Hunter JV, Haselgrove JC. Changes in brain water diffusion during childhood. *Neuroradiology*. 1999;**41**:929-34. PubMed PMID: 10639670.
 13. Sener RN. Diffusion MRI: apparent diffusion coefficient (ADC) values in the normal brain and a classification of brain disorders based on ADC values. *Comput Med Imaging Graph*. 2001;**25**:299-326. PubMed PMID: 11356324.
 14. Alexander AL, Tsuruda JS, Parker DL. Elimination of eddy current artifacts in diffusion-weighted echo-planar images: the use of bipolar gradients. *Magn Reson Med*. 1997;**38**:1016-21. PubMed PMID: 9402204.
 15. Dietrich O, Biffar A, Baur-Melnyk A, Reiser MF. Technical aspects of MR diffusion imaging of the body. *Eur J Radiol*. 2010;**76**:314-22. doi: 10.1016/j.ejrad.2010.02.018. PubMed PMID: 20299172.
 16. Le Bihan D, Breton E, Lallemand D, Grenier P, Cabanis E, Laval-Jeantet M. MR imaging of intravoxel incoherent motions: application to diffusion and perfusion in neurologic disorders. *Radiology*. 1986;**161**:401-7. doi: 10.1148/radiology.161.2.3763909.
 17. Berens ME, Rutka JT, Rosenblum ML. Brain tumor epidemiology, growth, and invasion. *Neurosurg Clin N Am*. 1990;**1**:1-18. PubMed PMID: 2135961.
 18. Mardor Y, Roth Y, Ochershvilli A, Spiegelmann R, Tichler T, Daniels D, et al. Pretreatment prediction of brain tumors' response to radiation therapy using high b-value diffusion-weighted MRI. *Neoplasia*. 2004;**6**:136-42. doi: 10.1593/neo.03349. PubMed PMID: 15140402. PubMed PMID: PMC1502089.
 19. Sinnaeve D. The Stejskal-Tanner equation generalized for any gradient shape—an overview of most pulse sequences measuring free diffusion. *Concepts in Magnetic Resonance Part A*. 2012;**40**:39-65. doi: 10.1002/cmr.a.21223.
 20. Mohamed FF, Ismail AAA, Hasan DI, Essa WE. The role of apparent diffusion coefficient (ADC) value in the differentiation between the most common pediatric posterior fossa tumors. *The Egyptian Journal of Radiology and Nuclear Medicine*. 2013;**44**:349-55. doi: 10.1016/j.ejrm.2012.12.011.
 21. Rumboldt Z, Camacho DL, Lake D, Welsh CT, Castillo M. Apparent diffusion coefficients for differentiation of cerebellar tumors in children. *AJNR Am J Neuroradiol*. 2006;**27**:1362-9. PubMed PMID: 16775298.
 22. Uysal F, Çakmakçı H, Yiş U, Ellidokuz H, Hız AS. Measurement of the apparent diffusion coefficient in paediatric mitochondrial encephalopathy cases and a comparison of parenchymal changes associated with the disease using follow-up diffusion coefficient measurements. *Eur J Radiol*. 2014;**83**:212-8. doi: 10.1016/j.ejrad.2013.06.031.
 23. Zitouni S, Koc G, Doganay S, Saracoglu S, Gumus KZ, Ciraci S, et al. Apparent diffusion coefficient in differentiation of pediatric posterior fossa tumors. *Jpn J Radiol*. 2017;**35**:448-53. doi: 10.1007/s11604-017-0652-9. PubMed PMID: 28550357.
 24. Pierce T, Kranz PG, Roth C, Leong D, Wei P, Provenzale JM. Use of apparent diffusion coefficient values for diagnosis of pediatric posterior fossa tumors. *Neuroradiol J*. 2014;**27**:233-44.

- doi: 10.15274/NRJ-2014-10027. PubMed PMID: 24750714. PubMed PMCID: PMC4202860.
25. Kotsenas AL, Roth TC, Manness WK, Faerber EN. Abnormal diffusion-weighted MRI in medulloblastoma: does it reflect small cell histology? *Pediatr Radiol.* 1999;**29**:524-6. doi: 10.1007/s002470050636. PubMed PMID: 10398789.
26. Jaremko JL, Jans LB, Coleman LT, Ditchfield MR. Value and limitations of diffusion-weighted imaging in grading and diagnosis of pediatric posterior fossa tumors. *AJNR Am J Neuroradiol.* 2010;**31**:1613-6. doi: 10.3174/ajnr.A2155. PubMed PMID: 20538820.
27. Filippi CG, Edgar MA, Ulug AM, Prowda JC, Heier LA, Zimmerman RD. Appearance of meningiomas on diffusion-weighted images: correlating diffusion constants with histopathologic findings. *AJNR Am J Neuroradiol.* 2001;**22**:65-72. PubMed PMID: 11158890.
28. Pillai S, Singhal A, Byrne AT, Dunham C, Cochrane DD, Steinbok P. Diffusion-weighted imaging and pathological correlation in pediatric medulloblastomas-"They are not always restricted!". *Childs Nerv Syst.* 2011;**27**:1407-11. doi: 10.1007/s00381-011-1499-5. PubMed PMID: 21732119.